



**Electronic structure of Rf<sup>+</sup> (Z = 104) from *ab initio* calculations**Harry Ramanantoanina <sup>1,2,\*</sup>, Anastasia Borschevsky,<sup>3</sup> Michael Block,<sup>1,2,4</sup> and Mustapha Laatiaoui <sup>1,2</sup><sup>1</sup>*Department Chemie, Johannes Gutenberg-Universität, Fritz-Strassmann Weg 2, 55128 Mainz, Germany*<sup>2</sup>*Helmholtz-Institut Mainz, Staudingerweg 18, 55128 Mainz, Germany*<sup>3</sup>*Van Swinderen Institute for Particle Physics and Gravity, University of Groningen, Nijenborgh 4, 9747 Groningen, The Netherlands*<sup>4</sup>*GSI Helmholtzzentrum für Schwerionenforschung, Planckstrasse 1, 64291 Darmstadt, Germany*

(Received 16 April 2021; accepted 29 July 2021; published 13 August 2021)

We report calculation of the energy spectrum and the spectroscopic properties of the superheavy element ion: Rf<sup>+</sup>. We use the four-component relativistic Dirac-Coulomb Hamiltonian and the multireference configuration interaction model to tackle the complex electronic structure problem that combines strong relativistic effects and electron correlation. We determine the energies of the ground and the low-lying excited states of Rf<sup>+</sup>, which originate from the  $7s^2 6d^1$ ,  $7s^1 6d^2$ ,  $7s^2 7p^1$ , and  $7s^1 6d^1 7p^1$  configurations. The results are discussed vis-à-vis the lighter homolog Hf<sup>+</sup> ion. We also assess the uncertainties of the predicted energy levels. The main purpose of the presented calculations is to provide a reliable prediction of the energy levels and to identify suitable metastable excited states that are good candidates for the planned ion-mobility-assisted laser spectroscopy studies.

DOI: [10.1103/PhysRevA.104.022813](https://doi.org/10.1103/PhysRevA.104.022813)**I. INTRODUCTION**

With the recent confirmation of four elements [1,2], the seventh row of the periodic table is now complete. Superheavy elements (SHEs) with atomic number  $Z > 103$  are part of the seventh period. They do not occur on earth but are synthesized in single atom-at-a-time quantities [3,4]. Moreover, they are short lived so that their experimental investigation is also very challenging. Recently, within the laser resonance chromatography (LRC) project [5], a great deal of attention became focused on developing element-selective spectroscopy that is conceptually dedicated to SHE ions. In the recently developed method, optical pumping of ions drifting in dilute helium is exploited to identify optical resonances. Successful excitation of ionic levels initiates pumping to metastable states and causes an abrupt change in the transport properties, which can be measured using drift time spectrometers [5,6]. However, to enable atomic structure investigations on systems that lack tabulated spectral lines, such experiments have to be pursued hand in hand with high-accuracy *ab initio* calculations.

Predicting energy levels, lifetimes, and branching ratios help scientists to quantify experimental parameters, such as the required detector sensitivities and beam times [7]. In a recent work [8], the energy spectrum of the SHE ion Lr<sup>+</sup> ( $Z = 103$ ) was predicted using the relativistic Fock space coupled cluster (FSCC) method and the configuration-interaction (CI) approach combined with many-body perturbation theory. The ground and the metastable excited states of Lr<sup>+</sup> stemming from the  $7s^2$  and  $6d^1 7s^1$  electron configurations, respectively, were identified together with the excitation scheme that is suitable for future LRC experiments [3]. In this paper, we are focusing our interest on the energy levels and the spec-

troscopic properties of the SHE ion Rf<sup>+</sup> ( $Z = 104$ ). The electronic structure of Rf is not trivial due to the complex combination of quantum interactions involving electron correlation, relativistic effects, and hyperfine structure [9,10]. Nonetheless, Rf has been in the spotlight of many theoretical investigations. Since the early 1990s, several studies have been devoted to predictions of its energy levels [11], atomic radii [12], ionization potentials [12], oxidation states, and chemical properties [13–16]. For the Rf<sup>+</sup> ion, to the best of our knowledge, very few theoretical data are found. FSCC calculations revealed the ground and some excited states belonging to the  $6d^1 7s^2$  and  $7s^2 7p^1$  configurations [17]. However, many levels were omitted, namely, those originating from the metastable  $6d^2 7s^1$  configuration due to the practical restriction of the FSCC method to systems of up to two valence electrons or holes, which leaves part of the Rf<sup>+</sup> energy spectrum out of the scope of this approach. Therefore, here we are, in particular, interested in going beyond the earlier work [17] by investigating the relative positions of the energy levels of the metastable  $6d^2 7s^1$  configuration, which are important for the development of optical pumping schemes for the Rf<sup>+</sup> ion in future LRC experiments [5,7].

The use of the CI model prevails as the most appropriate method for treating the Rf<sup>+</sup> ion system due to the fact that it can be applied to open shells that contain more than two valence particles and because of the straightforward approach to extracting the spectroscopic properties. In this paper, the theoretical results are obtained using the state-of-the-art relativistic approach *via* the four-component Dirac-Coulomb Hartree-Fock (DCHF) calculation complemented with a multireference configuration-interaction (MRCI) model as implemented in the DIRAC program package [18]. In MRCI, a subset of the full CI expansion is used to retrieve the correlation energy. In practice, only single and double excitations are retained up to the level of truncation of the CI expansion.

\*Corresponding author: [haramana@uni-mainz.de](mailto:haramana@uni-mainz.de)

MRCI models have been shown to yield accurate results for heavy and SHE elements with many applications available in the literature [19–21]. We preferred the molecular DIRAC package [18] over the available atomic codes [22–25] as it can be also used to study the Rf<sup>+</sup>-He interactions, which are very important for predicting transport properties of ions in gases [26]. Such calculations will constitute the next step in our investigations of the properties of Rf<sup>+</sup>. In order to assess the accuracy of the Rf<sup>+</sup> results, we also performed calculation of the properties of its lighter homolog, the Hf<sup>+</sup> ion, and compared our results with the experimental data that are systematically tabulated within the framework of the National Institute of Standards and Technology (NIST) spectral database [27].

## II. METHOD AND COMPUTATIONAL DETAILS

All the calculations were carried out using the DIRAC19 code [18] and were based on the four-component Dirac-Coulomb Hamiltonian. We used the finite-nucleus model in the form of a Gaussian charge distribution to treat the nuclei [28]. We have employed the Dyall basis sets for both elements [29,30]. Preliminary tests carried out in our paper showed that basis set expansion had a rather small effect on the energy levels (see also the Supplemental Material Table S1 [31]). It is noteworthy, however, to point that orbitals with higher angular momentum contribute to the energies in the alkali atoms [32]. Therefore, unless stated otherwise, all the results reported here were obtained using the dyall.cv3z basis sets, following the DIRAC19 nomenclature [18]. These basis sets consisted of uncontracted Gaussian-type orbitals for the large component wave function up to (30s24p15d11f4g1h) and (32s29p20d14f4g1h) for the Hf and Rf elements [29,30], respectively. The small component functions were generated from the large component basis set by strict kinetic balance [33]. We have also tested the singly and doubly augmented basis sets (s-aug-dyall.cv3z and d-aug-dyall.cv3z) by adding extra diffuse functions in an even-tempered manner; the augmentation also had only a small effects on the calculated energy levels (see the Supplemental Material Table S2 [31]).

The spherical symmetry of the atomic systems was reduced to the  $D_{\infty h}$  symmetry group as implemented in DIRAC19 [18]. In practice, the calculations used a subgroup of the axial rotation double group  $D_{32h}$ . In this double group, all  $m_j$  values fall into unique representations as long as  $m_j \leq 32$ . Therefore, the Fock matrix was block diagonalized in the orthonormal basis of the  $m_j$  quantum numbers [34]. The atomic spinors were selectively discriminated with respect to the representation  $\omega$ , including the  $m_j$  value and the parity. The atomic spinors that were used for the CI calculation (*vide infra*) were obtained by using the average of configuration- (AOC-) type calculation at the DCHF level of theory [35]. The AOC allowed us to represent the open-shell system with three valence electrons that were evenly distributed over 12 valence spinors (six Kramers pair) of  $s$  and  $d$  atomic characters. Thus, 68 and 100 electrons were restricted to closed shells for the Hf<sup>+</sup> and Rf<sup>+</sup> ions, respectively, whereas we used fractional occupation numbers (0.1250 = 3/12) for the merged Hf 6s-5d as well as Rf 7s-6d shells.

TABLE I. Specification of the GAS scheme used for the calculations on Hf<sup>+</sup> and Rf<sup>+</sup> (see the text for details).

GAS	Accumulated electrons		Number of Kramers pairs	Characters <sup>a</sup>
	min <sup>b</sup>	max		
1	10-x	10	5 (5/0)	(n-2)d
2	18-y	18	4 (1/3)	(n-1)s, (n-1)p
3	32-x	32	7 (0/7)	(n-2)f
4	32	35	9 (6/3)	ns, (n-1)d, np
5	35	35	102 (52/50)	Virtual

<sup>a</sup> $n$  is principal quantum number that represents the valence electrons' state of Hf<sup>+</sup> and Rf<sup>+</sup> ions, i.e. 6 and 7, respectively.

<sup>b</sup> $x-z$  are variables that control the electron excitation process attributed to the selective GAS.

The CI calculations were performed by using the Kramers-restricted configuration-interaction (KRCI) module in DIRAC19 [18]. KRCI was developed from string-based CI [36,37], the algorithm of which was fully operational within the four-component relativistic framework [34]. In DIRAC19 [18], the KRCI calculations use the concept of generalized active space (GAS) [38], which enables MRCI calculations with single- and double-electron excitations for different GAS setups [34]. The MRCI model a priori takes into consideration the dynamical correlation of the active electrons [39].

We report in Table I the GAS setup together with the technical specifications that were important in the MRCI calculation. For both Hf<sup>+</sup> and Rf<sup>+</sup> calculations, we placed within GAS 1–3 the 32 highest-lying fully occupied spinors (16 Kramers pairs) that formed the basis of the following representations:  $\omega = 1/2_g$  (3 Kramers pairs),  $3/2_g$  (2 Kramers pairs),  $5/2_g$  (1),  $(1/2_u)$  (4),  $3/2_u$  (3),  $5/2_u$  (2), and  $7/2_u$  (1). These spinors were predominantly of  $d$ ,  $s$ ,  $p$ , and  $f$  atomic characters. Furthermore, we placed within GAS 4 the 12 spinors with fractional electron occupation that formed the basis of the representations  $\omega = 1/2_g$  (three Kramers pairs),  $3/2_g$  (2) and  $5/2_g$  (1); as well as the six virtual spinors that formed the basis of the representations  $\omega = 1/2_u$  (two Kramers pairs) and  $3/2_u$  (1). These spinors were predominantly of valence  $s$ ,  $d$ , and  $p$  atomic characters. Finally, we placed within GAS 5 the 204 lowest-lying energy of virtual spinors (102 Kramers pairs) with energies below 30 atomic units.

Within the defined GAS setup, the MRCI model was designed to activate in total 35 electrons, a method that we referred to as MRCI(35). We defined the parameters  $x-z$  to control the electron excitation process that occurred at the semi-core level of Hf<sup>+</sup> and Rf<sup>+</sup> (Table I). These parameters took 0–2 values, which signified zero-, single-, and double-electron excitations allowed from the selective GAS. We requested the following number of roots in the MRCI calculations: 37, 32, 22, 12, 6, and 1 roots for representations with even-parity  $\Omega = 1/2_g$ ,  $(3/2_g, 5/2_g, 7/2_g, \text{ and } 9/2_g)$ , respectively; 25, 20, 12, 5, and 1 roots for representations with odd-parity  $\Omega = 1/2_u$ ,  $3/2_u, 5/2_u, 7/2_u, 9/2_u, \text{ and } 11/2_u$ , respectively. The large number of roots were needed due to many

near-degenerate electronic states that we found in the energy range between 0 and 50 000 cm<sup>-1</sup> for both Hf<sup>+</sup> and Rf<sup>+</sup> ions.

### III. RESULTS AND DISCUSSION

#### A. Energy levels

The MRCI method is in practice limited by the choice of basis sets and the number of correlated electrons. It, thus, becomes important to investigate the effect of the basis set quality on the calculated energy levels of the Hf<sup>+</sup> ion in order: to pursue the basis set limit at a reasonable computational cost; and to ensure that uncertainties are maintained at acceptable levels. In the Supplemental Material (Table S1) [31], we report the calculated energies as a function of the basis sets quality. These multiplet energies include the ground-state  $^2D_{3/2}$  ( $5d^16s^2$ ), the low-lying excited states  $^2D_{3/2}$  ( $5d^16s^2$ ), and  $^4F_{3/2}$  ( $5d^16s^16p^1$ ), which were selected to represent the whole manifold of the low-lying Hf<sup>+</sup> electronic levels. We used the uncontracted Dyal basis sets of double- (cv2z), triple- (cv3z), and quadruple- $\zeta$  (cv4z)  $\zeta$  quality including valence-correlating and core-valence correlating functions [29]. The quadruple- $\zeta$  basis sets are also characterized by the presence of higher angular momentum up to  $l = 6$   $i$  functions. By increasing the basis set quality (from double  $\zeta$  to quadruple  $\zeta$ ), we only obtained a small effect on the calculated energy levels with the estimated standard deviations of the energies in the magnitude of tens of cm<sup>-1</sup> (see Table S1 of the Supplemental Material [31]). Further augmentation by single and double diffuse functions at the triple- $\zeta$  basis set level is also found to have only a minor effect on the atomic energy levels with the estimated standard deviations of the calculated energies ranging from less than 3 to 15 cm<sup>-1</sup> (see Supplemental Material, Table S2 [31]). Therefore, the uncertainties of the calculation due to basis set expansion and quality are small. We have, thus, selected the core-valence correlating triple- $\zeta$  basis set also for consistency with earlier studies of analogous elements. For example, Fleig and Nayak [40] reported similar MRCI calculations of the HfF<sup>+</sup> molecule using basis sets of triple- $\zeta$  quality.

We also investigated the effect of the semi-core-electron excitations on the energy levels of the Hf<sup>+</sup> ion. Although we are fundamentally interested in the ground and low-lying excited states that belong to the active space of the Hf  $5d$ ,  $6s$ , and  $6p$  orbitals, early CI studies recommended the consideration of core electrons [40]. To study this, we performed calculations in which the parameters  $x$ - $z$  in Table I are varied. Since  $x$ - $z$  cannot be equal or higher than three (technically possible but generating a massive number of Slater determinants that are beyond the scope of our computational resources), we excluded this situation from the MRCI calculation. In Supplemental Material Table S3 [31], we report the calculated multiplet energies as a function of the  $x$ - $z$  variables. We did not find major energy changes when up to one electron excitation is allowed from GAS 1 (i.e.,  $x = 1$ ). However, by allowing single- and double-electron excitation from GAS 2 (i.e.,  $y = 2$ ), the energies of the states that have even parity were generally improved in relation to the experimental values. Moreover, we also found that the energies of the states with odd parity were shifted to higher values

with better agreement with the experiments when one-electron excitations were allowed in GAS 3 (i.e.,  $z = 1$ ). Based on this paper, MRCI(35) with  $x = 0$ ,  $y = 2$ , and  $z = 1$  is our method of choice. This computational setup explicitly treats correlation effects of 35 electrons, whereas the CI space contains the  $(5d, 6s, 6p)^3$  configurations with up to two holes in Hf  $5s$  and  $5p$  and one hole in Hf  $4f$ .

We report in Table II the calculated excitation energies of Hf<sup>+</sup> obtained using the MRCI(35) model together with known experimental values for comparison [41]. Only levels with energies below 40 000 cm<sup>-1</sup> are listed for convenience. We have analyzed the natural orbital occupation numbers of the CI vectors to classify the states and to identify their dominant electron configurations. In order to correct our results for the Breit and the lowest-order QED contributions [42], we used the GRASP program package [23], which is based on the Dirac-Coulomb-Breit Hamiltonian and the multiconfiguration Dirac-Fock (MCDF) model and incorporates the lowest-order QED corrections, i.e., the vacuum polarization and the self-energy terms. Details for the implementation of the Breit and QED corrections in GRASP [23] can be found elsewhere [23,43,44]. The reference space for the MCDF CI calculation was the  $4f^{14}(5d6s6p)^3$  multiplet manifold. The core  $5s$  and  $5p$  electrons were also correlated, and they produced an average shift in the transition energies of only a few cm<sup>-1</sup>. The virtual space for the CI expansion consisted in one extra spinor for each  $l$  quantum number from 0 to 4 (i.e.,  $7s7p6d5f5g$ ). It was also found that the calculated Breit and QED corrections were relatively independent of the size of the CI expansion, and they remained very close to the values listed in Table II. The values in Table II represent the differences in energy calculated at the Dirac-Coulomb and Dirac-Coulomb-Breit level of theory ( $\Delta_B$ ) and the difference between the Dirac-Coulomb-Breit and the Dirac-Coulomb-Breit + QED values ( $\Delta_{B+QED}$ ). We found that the Breit and QED corrections are relatively small on the order of 100 cm<sup>-1</sup> for Hf<sup>+</sup> and comparable with the Breit and QED effects calculated for analogous  $3d$  elements [8,42,45]. Based on the calculated MRCI energy data together with the Breit and QED corrections, we obtain the recommended energy values for Hf<sup>+</sup> that are also listed in Table II.

The Hf<sup>+</sup> ground and low-lying excited states belong to the configurations  $5d^16s^2$ ,  $5d^26s^1$ , and  $5d^3$  that have even parity as well as configurations  $5d^16s^16p^1$  and  $5d^26p^1$  that have odd parity. We also find that the multiplets corresponding to the  $6s^26p^1$  configuration are definitely above 50 000 cm<sup>-1</sup>. The ground state is fourfold degenerate with  $J = 3/2$  that arise from the spin-orbit coupling of the  $^2D$  term of configuration  $5d^16s^2$ . The mean percentage error for the states that belong to the  $5d^26s^1$  configuration is relatively small (< 5%). We found larger errors for the states originating in the configuration where the three electrons occupy different orbitals ( $5d^16s^16p^1$ ). Overall, the calculated energy levels of Hf<sup>+</sup> are in good agreement with the NIST values [41], confirming the suitability of the MRCI model for this paper.

However, we should point out that the calculated spin-orbit splitting of the  $^2D$  ground state, which is off by 200 cm<sup>-1</sup>, is somewhat intriguing (see Table II). We have tested the possibility that the error stems from the use of the AOC procedure in the DCHF calculation (the Method section). We

TABLE II. Calculated energies (in  $\text{cm}^{-1}$ ) of the low-lying excited states of the  $\text{Hf}^+$  ion together with the recommended values (Final) that take into consideration the Breit ( $\Delta_B$ ) and QED ( $\Delta_{B+QED}$ ) corrections, classified with respect to the dominant electron configuration (Config.) and compared with the experimental values (Expt.).

Config.	State	$J$	Expt.	Theory			Final	
				MRCI	$\Delta_B$	$\Delta_{B+QED}$		
$5d^16s^2$	$^2D$	3/2	0	0			0	
		5/2	3051	2850	-67	-5	2845	
$5d^26s^1$	$^4F$	3/2	3642	3970	101	-95	3875	
		5/2	4905	4913	63	-92	4821	
		7/2	6344	6165	19	-93	6072	
		9/2	8362	7835	-43	-90	7745	
		1/2	11952	11745	46	-96	11649	
	$^4P$	3/2	12921	12976	11	-93	12883	
		5/2	13486	13396	0.1	-91	13305	
		7/2	15085	14480	-16	-100	14380	
	$^2F$	5/2	12071	12227	65	-100	12127	
		7/2	15085	14480	-16	-100	14380	
	$^2D$	3/2	14360	14430	34	-106	14324	
		5/2	17369	16834	-74	-84	16750	
	$^2P$	1/2	15255	15366	37	-133	15233	
		3/2	17830	17945	-56	-118	17827	
	$^2G$	9/2	17389	17394	-24	-106	17288	
7/2		17711	18100	-24	-108	17992		
$5d^3$	$^2S$	1/2		21117	-87	-95	21022	
		3/2	18898	19605	138	-221	19384	
	$^4F$	5/2	20135	20560	95	-220	20340	
		7/2	21638	21745	44	-217	21528	
		9/2	23146	23023	-6	-215	22808	
	$^4P$	1/2	26997	27689	61	-218	27471	
		3/2	27285	27930	56	-217	27713	
		5/2	28547	28933	12	-217	28716	
	$5d^16s^16p^1$	$^4F$	3/2	28069	27320	9	-89	27231
			5/2	29405	28666	-1	-97	28569
7/2			33776	32484	-97	-82	32402	
9/2			38186	36836	-161	-78	36758	
1/2			29160	28713	-50	-56	28657	
$^4D$		3/2	31784	31214	-97	-81	31133	
		5/2	34355	33549	-63	-90	33459	
		7/2	36882	35578	-100	-84	35494	
$^2D$		5/2	33181	32390	-75	-100	32290	
		3/2	34124	33174	-17	-98	33076	
$^2P$		1/2	33136	32693	-41	-145	32548	
		3/2	36373	35973	-82	-139	35834	
$^2D$		3/2	37886	38237	-92	-187	38050	
		5/2	41761	41313	-121	-172	41141	
$^2F$		5/2	38579	37873	-54	-126	37747	
	7/2	41407	40840	-97	-125	40715		
$^4P$	1/2	38399	38271	-56	-82	38189		
	3/2	39227	38546	-100	-70	38476		
	5/2	40507	39585	-129	-107	39478		
$5d^26p^1$	$^4G$	5/2	34943	34585	10	-168	34417	
		7/2	38499	37751	-29	-195	37556	

carried out an additional test by changing the fractional occupation scheme of the  $\text{Hf } 6s$  and  $5d$  orbitals, the AOC itself being necessary to populate unpaired electrons on degenerate spinors. We eventually found out that by placing two electrons in  $6s$  (in other words, taking  $6s$  as a closed shell) and one

TABLE III. Calculated energies (in  $\text{cm}^{-1}$ ) of the low-lying excited states of  $\text{Rf}^+$  ion together with the recommended values (Final) that take into consideration the Breit ( $\Delta_B$ ) and QED ( $\Delta_{B+QED}$ ) corrections, classified with respect to the dominant electron configuration (Config.).

Config.	State	$J$	Theory			Final
			MRCI	$\Delta_B$	$\Delta_{B+QED}$	
$6d^17s^2$	$^2D$	3/2	0			0
		5/2	5682	-177	-2	5680
$6d^27s^1$	$^4F$	3/2	15931	94	-253	15678
		5/2	17642	42	-250	17392
		7/2	20476	-71	-245	20231
		9/2	23621	-172	-239	23382
		1/2	24864	13	-249	24615
$^4P$	3/2	26993	-35	-245	26648	
	5/2	29832	-74	-245	29587	
	7/2	32631	-225	-255	32376	
$^2F$	5/2	26820	-69	-255	26565	
	7/2	32631	-225	-255	32376	
$^2D$	3/2	30245	-77	-262	29983	
	5/2	34515	-244	-236	34279	
$^2P$	1/2	32851	-49	-301	32550	
	3/2	36860	-210	-290	36570	
$^2G$	9/2	34267	-156	-257	34010	
	7/2	36615	-98	-254	36361	
$^2S$	1/2	44529	-261	-233	44296	
	3/2	16691	-122	-34	16657	
$7s^27p^1$	$^2P$	1/2	16691	-122	-34	16657
		3/2	31288	-223	-47	31241
$6d^17s^17p^1$	$^4F$	3/2	28052	-44	-206	27846
		5/2	31244	-77	-213	31031
		7/2	38140	-252	-197	37943
		9/2	50467	-399	-199	50268
		1/2	36338	-87	-182	36156
	$^4D$	3/2	39040	-192	-226	38814
		5/2	42676	-169	-266	42410
		7/2	47934	-248	-197	47737
	$^2D$	5/2	37601	-220	-203	37398
		3/2	42421	-227	-226	42195
$^2F$	5/2	46318	-195	-266	46052	
	7/2	55434	-252	-379	55055	
$^2D$	3/2	48008	-160	-204	47804	
	5/2	53780	-180	-279	53501	
$^4P$	1/2	48374	-193	-210	48164	
	3/2	50577	-193	-314	50263	
	5/2	51921	-300	-345	51576	

electron in  $5d_{3/2}$  (in a fractional manner), the spin-orbit splitting of the  $\text{Hf}^+ ^2D$  ground state equaled  $2910 \text{ cm}^{-1}$ , a value which was very close to the experimental data. However, all the energy levels of the  $5d^26s^1$  configuration were shifted to higher-energy values as a side effect. We, thus, proceeded with the original AOC scheme.

We report in Table III the excitation energies of  $\text{Rf}^+$  calculated by means of the MRCI(35) methodology. For convenience, only levels with energies below  $50\,000 \text{ cm}^{-1}$  are listed. The spin-orbit coupling interactions of the  $6d$ ,  $7s$ , and  $7p$  electrons are much larger than for  $\text{Hf}^+$ , and the energy spectrum is rather more sparse. We have also performed a similar analysis to account for the Breit and the QED



contributions as was performed for the Hf<sup>+</sup> ion using the MCDF calculation in GRASP [23]. The reference space for the MCDF CI calculation was the  $5f^{14}(6d7s7p)^3$  multiplet manifold. The core  $6s$  and  $6p$  electrons were also correlated. The virtual space for the CI expansion consisted in one extra spinor for each  $l$  quantum number from 0 to 2, together with two extra spinors for each  $l$  quantum number from 3 to 5 and the  $6h$  function (i.e.,  $8s8p7d6f7f5g6g6h$ ). The Breit and QED contributions approximately double going from Hf<sup>+</sup> to Rf<sup>+</sup> ions and are on the order of 200 cm<sup>-1</sup> (see Table III) for most levels, in good agreement with calculated QED effects for the analogous SHE elements [8,42,46,47]. The recommended energy values for Rf<sup>+</sup> are also listed in Table III based of the calculated MRCI energy data together with the Breit and QED corrections.

We identify the multiplet terms from configurations  $6d^17s^2$ ,  $6d^27s^1$ , and  $7s^27p^1$  as the ground and low-lying excited states. In particular, the two spin-orbit components of the  $^2P$  state ( $7s^27p^1$ ) are predicted to reside at a much lower energy than in Hf<sup>+</sup>. Similar to Hf<sup>+</sup>, the calculated ground state of Rf<sup>+</sup> is  $^2D_{3/2}$  from the  $6d^17s^2$  configuration, and the first low-lying excited state is its spin-orbit counterpart ( $^2D_{5/2}$ ) at 5682 cm<sup>-1</sup>. The second low-lying excited state is the metastable state ( $^4F_{3/2}$ ) that forms the basis of the  $6d^27s^1$  configuration. Above this level, we obtain the third excited state that is a term with odd parity ( $^2P_{1/2}$  from configuration  $7s^27p^1$ ). The energy difference between this latter and the metastable state is predicted to be 761 cm<sup>-1</sup>.

The definition of the second and third excited states in the Rf<sup>+</sup> energy spectrum is critical in the setup of the ion-mobility-assisted laser spectroscopy studies (*vide infra*). In particular, the relative position of the  $^2P_{1/2}$  odd level with respect to the  $^4F_{3/2}$  metastable state could determine the feasibility of one of the proposed pumping schemes, see below. To evaluate the energy uncertainty for these levels from a theoretical perspective, we used the Fock space coupled cluster (FSCC) method [48,49]. However, we note once again that FSCC is currently not applicable for all the states of interest in Rf<sup>+</sup>, and we, thus, focus on those states that can be reached with this method. The FSCC calculation was also carried out using the DIRAC19 code, and the computational details were kept, inasmuch as possible, similar to the present MRCI method for consistency. We started with a relativistic DCHF calculation of the Rf<sup>2+</sup> ion because the valence electron operator in the FSCC is defined with respect to a closed-shell reference [48,49]. Then all the closed-shell electrons were correlated, and virtual orbitals were also included up to +30 atomic units. Finally, one electron was added in order to obtain Rf<sup>+</sup>, and the coupled cluster equations were solved accordingly. Within the FSCC nomenclature, we have applied sector (0,1) with respect to the closed-shell reference, where 0 signifies 0 holes in the  $7s$  valence orbital and 1 signifies one valence electron that is allowed to occupy the Rf  $6d$  and  $7p$  orbitals. Thus, only excitation energies that result from the  $6d^17s^2$  and  $7s^27p^1$  configurations could be evaluated.

The calculated FSCC energies of the spin-orbit components of the  $^2P$  terms (configuration  $7s^27p^1$ ) are equal to 17 535 and 33 785 cm<sup>-1</sup> when using the triple- $\zeta$  basis set. The same energies became 18 216 and 34 502 cm<sup>-1</sup> upon switching to the quadruple- $\zeta$  basis set. These levels, thus,

present basis set dependency but they remained definitely at a higher energy than the MRCI  $^2P$  results listed in Table III. For the  $^2D_{5/2}$  level (configuration  $6d^17s^2$ ), the FSCC energy equaled 7064 and 7334 cm<sup>-1</sup>, respectively, by using the triple- and quadruple- $\zeta$  basis sets; also significantly higher than the MRCI predictions. In another FSCC study of Rf<sup>+</sup>, dated back to 1995 [17], the authors have used a very large basis set, but they have considered only correlation of 34 external electrons. Furthermore, they studied electron correlation effects by varying the size of the active space of virtual orbitals that were included in their calculation. The reported energy of the  $^2P_{1/2}$  state is within the 17 300–19 400-cm<sup>-1</sup> range, whereas the  $^2P_{3/2}$  is within 34 290–35 381 cm<sup>-1</sup>, and the  $^2D_{5/2}$  is calculated at approximately 7300 cm<sup>-1</sup>, in good agreement with the present FSCC calculations. From the estimated standard deviation of the energies that are obtained using the MRCI and the FSCC methods, we can derive the uncertainties of the  $^2D_{5/2}$ ,  $^2P_{1/2}$ , and  $^2P_{3/2}$  states as follows (in cm<sup>-1</sup>):  $5682 \pm 1382$ ,  $16\,691 \pm 844$ , and  $31\,283 \pm 2502$ , respectively.

What is striking, though, is that the calculated uncertainties are relatively large for the states that are mainly driven by the spin-orbit coupling interaction. The FSCC energy separation between the  $^2P_{1/2}$  and  $^2P_{3/2}$  states is 10% larger than that reported in Table III [we obtain 14 600 cm<sup>-1</sup> (MRCI) versus 16 250 cm<sup>-1</sup> (FSCC)]. Similarly, the energy separation between the  $^2D_{3/2}$  and the  $^2D_{5/2}$  states is found 25% higher for FSCC compared to the MRCI results reported in Table III [7064 cm<sup>-1</sup> (FSCC) versus 5682 cm<sup>-1</sup> (MRCI)]. It is possible that the *modus operandi* of the FSCC calculation produces overestimation of the energies due to the fact that it does not account for the mixing with the three-valence electron configurations.

## B. Spectroscopic properties

The electronic states that originate from the configurations  $(n-1)d^1ns^1np^1$  and  $ns^2np^1$  decay *via* electric dipole  $E1$  mechanism for both Hf<sup>+</sup> (with  $n = 6$ ) and Rf<sup>+</sup> (with  $n = 7$ ) ions. However, the electronic states that originate from the configurations  $(n-1)d^1ns^2$  and  $(n-1)d^2ns^1$  decay only *via* electric quadrupole  $E2$  and magnetic dipole  $M1$  mechanisms. We calculated the inter- and intraconfiguration transition probabilities by using a phenomenological effective Hamiltonian. By means of the *ab initio* MRCI method, the relativistic form of the transition moment operator was also used to derive transition probabilities at the  $E1$  level. But, we did not obtain the transition probabilities of  $E2$  and  $M1$  transitions from *ab initio* calculations; instead, we have turned to the effective Hamiltonian approach. It is noteworthy that the effective Hamiltonian method constitutes a semiempirical approach for spectroscopic properties. The results are based upon a mathematical least-squares fit of the *ab initio* energy levels and thereby produce qualitative transition probabilities that are sufficient to develop optical pumping scenarios for the Rf<sup>+</sup> ion (see Sec. III C). We use the quantum theory of Slater [35] where the matrix elements of the effective Hamiltonian are built based on perturbation theory and the central field approximation.

Slater's theory is described in detail in many texts [35,50,51], and we give here only a brief overview. The energies and the eigenvectors of any spectroscopic states of a system with  $N$  electrons are generally obtained from the diagonalization of the matrix elements of the atomic Dirac-Coulomb Hamiltonian (in atomic units),

$$H = \sum_i^N h_D(i) + \sum_{i<j}^N \left( \frac{1}{r_{ij}} \right), \quad (1)$$

where  $h_D$  and  $1/r_{ij}$  express the one- and two-electron operators, respectively. The one-electron Dirac operator consists of the kinetic energy and electron-nuclei attraction terms. The two-electron operator, on the other hand, includes the Coulomb-repulsion ( $J$ ) and the exchange ( $K$ ) integrals between electrons  $i$  and  $j$ . In Slater's theory for atomic calculations,  $1/r_{ij}$  is expanded with respect to spherical harmonics so that the  $J$  and  $K$  integrals can be separately discriminated into parts according to the spin, angular, and radial components. We use this definition to construct our effective Hamiltonian ( $H_{\text{eff}}$ ), and, therefore, transform Eq. (1) as follows:

$$H_{\text{eff}} = \sum_i^N h_0(i) + \sum_i^N \zeta_i l_i s_i + \sum_{i<j}^N \sum_k [F_k^k(n_i l_i, n_j l_j) f_k(l_i m_{l_i}, l_j m_{l_j}) - \delta_k(m_{s_i}, m_{s_j}) G_k^k(n_i l_i, n_j l_j) g_k(l_i m_{l_i}, l_j m_{l_j})], \quad (2)$$

where the first and the second terms on the right-hand side of the equation represent the one-electron operators including the spin-orbit coupling [52], whereas the third term represents the two-electron operator. In this latter, the terms  $f_k$ ,  $g_k$ , and  $\delta_k$  (with  $k$  being the multipole index) arise from the integration over the spin and angular components of the wave functions; the terms  $F_k$  and  $G_k$  are conventionally referred as the Slater-Condon integrals and result from the integration over the radial component [51].

By using Eq. (2), the effective Hamiltonian can be simply parametrized by the Slater-Condon integrals ( $F_k$  and  $G_k$ ) and spin-orbit coupling constants ( $\zeta_i$ ) [51], which allows us to operate the CI algorithm in a semiempirical manner. We note, however, that the parameters can be numerically evaluated, and there are numerous examples in the literature for dealing with lanthanides [51,53,54] or heavier actinide elements [55–57]. For the  $\text{Hf}^+$  and  $\text{Rf}^+$  ions, we constructed the effective Hamiltonian with  $N = 3$  electrons in the  $s$ ,  $d$ , and  $p$  valence orbitals. In this case, the size of the matrix elements of the effective Hamiltonian in Eq. (2) equaled  $816 \times 816$ , which was the dimension of the Hilbert space spanned by the CI problem of three electrons in 18 spinors. Moreover, the summation over the multipole index  $k$  did not exceed 4 in Eq. (2) [51]. Then, the Slater-Condon integrals and spin-orbit coupling constants are calculated by least-squares fit methods by minimizing the residual between the theoretical energies listed in Tables II and III (our reference energy values) and the calculated energies from the effective Hamiltonian. The least-squares fit is implemented using the FMINSEARCH tool in

TABLE IV. Calculated Einstein coefficients [ $A_{E1}$  ( $\text{s}^{-1}$ )] and branching ratios ( $\beta$ ) for the  $\text{Hf}^+$  ion, compared with the experimental data.

Upper level	Lower level	$A_{E1}$ Expt.	$A_{E1}$	$\beta$
$5d^1 6s^1 6p^1 \ ^4F_{3/2}$	$5d^1 6s^2 \ ^2D_{3/2}$		$1.271 \times 10^7$	0.520
	$5d^1 6s^2 \ ^2D_{5/2}$		$1.828 \times 10^4$	0.000
	$5d^2 6s^1 \ ^4F_{3/2}$		$1.068 \times 10^7$	0.437
	$5d^2 6s^1 \ ^4F_{5/2}$		$5.902 \times 10^2$	0.000
$5d^1 6s^1 6p^1 \ ^4F_{5/2}$	$5d^1 6s^2 \ ^2D_{3/2}$	$3.100 \times 10^7$	$1.953 \times 10^7$	0.552
	$5d^1 6s^2 \ ^2D_{5/2}$		$4.894 \times 10^6$	0.138
	$5d^2 6s^1 \ ^4F_{3/2}$		$3.455 \times 10^6$	0.098
	$5d^2 6s^1 \ ^4F_{5/2}$		$5.362 \times 10^6$	0.152
	$5d^2 6s^1 \ ^2D_{5/2}$		$1.561 \times 10^5$	0.004
$5d^1 6s^1 6p^1 \ ^4F_{7/2}$	$5d^1 6s^2 \ ^2D_{5/2}$	$2.100 \times 10^7$	$7.554 \times 10^6$	0.246
	$5d^2 6s^1 \ ^4F_{5/2}$		$3.920 \times 10^6$	0.128
	$5d^2 6s^1 \ ^4F_{7/2}$		$1.674 \times 10^7$	0.545
	$5d^2 6s^1 \ ^4F_{9/2}$		$1.518 \times 10^6$	0.049

MATLAB [58]. We report in the Supplemental Material Tables S4 and S5 [31] the calculated energies obtained from the effective Hamiltonian and compared with the reference values. The mathematical fit is well suited for well-separated energy levels; thus, the discrepancies between the reference energies and the effective Hamiltonian are larger for  $\text{Hf}^+$  than  $\text{Rf}^+$  (see Tables S4 and S5 in the Supplemental Material [31]).

We obtain the oscillator strengths using the following equations (in atomic units):

$$f_{i,j}^{(E1)} = \frac{2}{3} [E(j) - E(i)] \sum_{\alpha} |\langle \psi_j | D_{\alpha} | \psi_i \rangle|^2, \quad (3)$$

$$f_{i,j}^{(M1)} = \frac{2}{3} \alpha^2 [E(j) - E(i)] \sum_{\alpha} |\langle \psi_j | M_{\alpha} | \psi_i \rangle|^2, \quad (4)$$

$$f_{i,j}^{(E2)} = \frac{1}{20} \alpha^2 [E(j) - E(i)]^3 \sum_{a,b} |\langle \psi_j | Q_{ab} | \psi_i \rangle|^2, \quad (5)$$

where  $D_{\alpha}$ ,  $Q_{ab}$ , and  $M_{\alpha}$  are the electric dipole moment operator and the electric quadrupole tensor, which are formulated in the length gauge, and the magnetic dipole moment operator, respectively; the terms within the bra-ket notations represent the transition probabilities between states  $i$  and  $j$ , referring to the lower and upper levels of the electronic transitions.  $E$  and  $\psi$  are the calculated energies and eigenfunctions of the effective Hamiltonian. In Eqs. (4) and (5),  $\alpha = 1/137$  denotes the fine-structure constant. We derived the Einstein coefficients  $A_{E1}$ ,  $A_{M1}$ , and  $A_{E2}$  from the calculated transition probabilities using Eqs. (S1–(S3) in the Supplemental Material [31], respectively.

We report in Tables IV and V the calculated Einstein coefficients and the branching ratios of the  $E1$  atomic radiative transitions of the  $\text{Hf}^+$  and  $\text{Rf}^+$  ions, respectively. For clarity, we list only transitions that have potential implication in the optical pumping process of the LRC experiment [3]. The levels include the spin-orbit manifolds of  $^2D [(n-1)d \ ^1n s^2]$  with  $n = 6$  and  $7$  for  $\text{Hf}^+$  and  $\text{Rf}^+$ , respectively, as well as the low-lying metastable states  $^4F [(n-1)d \ ^2n s^1]$  and the low-lying bright excited states  $^4F [(n-1)d \ ^1n s \ ^1n p^1]$  and  $^2P (7s^2 7p^1)$ . For the  $\text{Hf}^+$  ion, the only two experimental

TABLE V. Calculated Einstein coefficients [ $A_{E1}$  ( $s^{-1}$ )] and branching ratios ( $\beta$ ) for the Rf<sup>+</sup> ion.

Upper level	Lower level	$A_{E1}$	$\beta$
$7s^2 7p^1$	${}^2P_{1/2}$ $6d^1 7s^2$ ${}^2D_{3/2}$	$1.089 \times 10^8$	0.977
	$6d^2 7s^1$ ${}^4F_{3/2}$	$2.530 \times 10^6$	0.023
$6d^1 7s^1 7p^1$	${}^4F_{3/2}$ $6d^1 7s^2$ ${}^2D_{3/2}$	$1.633 \times 10^8$	0.783
	$6d^1 7s^2$ ${}^2D_{5/2}$	$7.404 \times 10^6$	0.036
	$6d^2 7s^1$ ${}^4F_{3/2}$	$3.575 \times 10^7$	0.171
	$6d^2 7s^1$ ${}^4F_{5/2}$	$1.965 \times 10^6$	0.009
	$6d^2 7s^1$ ${}^4P_{1/2}$	$8.039 \times 10^4$	< 0.001
	$6d^2 7s^1$ ${}^2F_{5/2}$	$1.026 \times 10^5$	< 0.001
	$6d^2 7s^1$ ${}^4P_{3/2}$	$9.612 \times 10^4$	< 0.001
$6d^1 7s^1 7p^1$	${}^4F_{5/2}$ $6d^1 7s^2$ ${}^2D_{3/2}$	$2.415 \times 10^8$	0.535
	$6d^1 7s^2$ ${}^2D_{5/2}$	$1.212 \times 10^8$	0.268
	$6d^2 7s^1$ ${}^4F_{3/2}$	$2.585 \times 10^7$	0.057
	$6d^2 7s^1$ ${}^4F_{5/2}$	$5.928 \times 10^7$	0.131
	$6d^2 7s^1$ ${}^4F_{7/2}$	$2.394 \times 10^6$	0.005
	$6d^2 7s^1$ ${}^2F_{5/2}$	$1.312 \times 10^6$	0.003
	$6d^2 7s^1$ ${}^4P_{3/2}$	$5.521 \times 10^4$	< 0.001
	$6d^2 7s^1$ ${}^4P_{5/2}$	$5.504 \times 10^4$	< 0.001
	$6d^2 7s^1$ ${}^2D_{3/2}$	$1.653 \times 10^5$	< 0.001

values that are available from the literature are added in Table IV for comparison [41]. We found that the calculated Einstein coefficients are underestimated when compared to the experimental values, but the relative strengths of the electric dipole transitions are well reproduced. The strongest transitions are  ${}^2D_{3/2} \rightarrow {}^4F_{5/2}$  for both Hf<sup>+</sup> and Rf<sup>+</sup> ions. In order to get an additional check on the presented predictions, the electric dipole transition probabilities were also computed using the *ab initio* MRCI scheme in the DIRAC19 program package [18]. In the Supplemental Material Figs. S1 and S2 [31] show the simulated absorption spectra of both Hf<sup>+</sup> and Rf<sup>+</sup> ions, respectively, as they are determined with the *ab initio* and the effective Hamiltonian methods, revealing the consistency between the two theoretical models.

We report in Table VI the Einstein coefficients that are obtained from the electric quadrupole ( $E2$ ) and magnetic

TABLE VI. Calculated Einstein coefficients [ $A_{M1}$  and  $A_{E2}$  ( $s^{-1}$ )] for the magnetic dipole ( $M1$ ) and electric quadrupole ( $E2$ ) transitions, respectively, of the Rf<sup>+</sup> ion.

Upper level	Lower level	$A_{M1}$	$A_{E2}$
$6d^1 7s^2$	${}^2D_{5/2}$ $6d^1 7s^2$ ${}^2D_{3/2}$	1.480	$1.445 \times 10^{-3}$
$6d^2 7s^1$	${}^4F_{3/2}$ $6d^1 7s^2$ ${}^2D_{3/2}$	$3.165 \times 10^{-2}$	$1.833 \times 10^{-2}$
	$6d^1 7s^2$ ${}^2D_{5/2}$	$5.159 \times 10^{-2}$	$3.051 \times 10^{-6}$
$6d^2 7s^1$	${}^4F_{5/2}$ $6d^1 7s^2$ ${}^2D_{3/2}$	$5.001 \times 10^{-4}$	$1.714 \times 10^{-1}$
	$6d^1 7s^2$ ${}^2D_{5/2}$	$1.676 \times 10^{-2}$	$1.641 \times 10^{-5}$
	$6d^2 7s^1$ ${}^4F_{3/2}$	$1.005 \times 10^{-1}$	$2.094 \times 10^{-6}$
$6d^2 7s^1$	${}^4F_{7/2}$ $6d^1 7s^2$ ${}^2D_{3/2}$		$3.556 \times 10^{-3}$
	$6d^1 7s^2$ ${}^2D_{5/2}$	$1.294 \times 10^{-1}$	$1.011 \times 10^{-2}$
	$6d^2 7s^1$ ${}^4F_{3/2}$		$1.858 \times 10^{-6}$
$6d^2 7s^1$	${}^4F_{5/2}$ $6d^2 7s^1$ ${}^4F_{3/2}$	$1.294 \times 10^{-1}$	$3.174 \times 10^{-5}$
	$6d^1 7s^2$ ${}^2D_{5/2}$		$1.339 \times 10^{-2}$
	$6d^2 7s^1$ ${}^4F_{5/2}$		$1.077 \times 10^{-4}$
$6d^2 7s^1$	${}^4F_{7/2}$ $6d^2 7s^1$ ${}^4F_{7/2}$	$4.509 \times 10^{-1}$	$1.832 \times 10^{-5}$

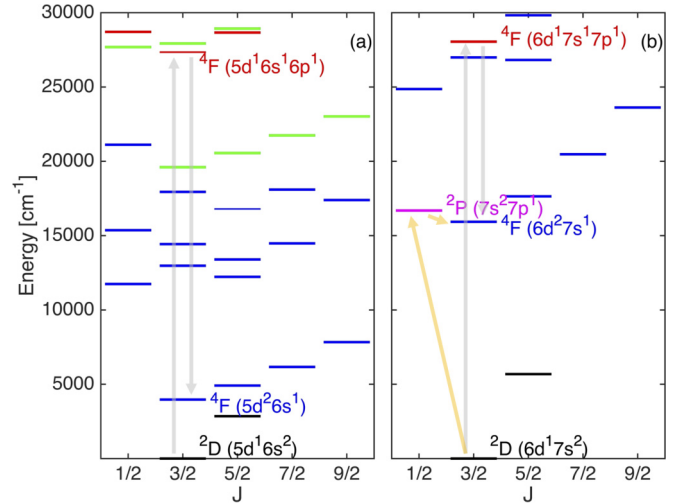


FIG. 1. Graphical representation of selected energy levels, showing the ground and the low-lying excited states with predominant configurations  $(n-1)d^1(n)s^2$  (in black);  $(n-1)d^2(n)s^1$  (in blue);  $(n-1)d^3$  (in green);  $(n-1)d^1(n)s^1(n)p^1$  (in red); and  $(n-1)d^1(n)s^1(n)p^1$  (in magenta) of Hf<sup>+</sup> (a) and Rf<sup>+</sup> (b) ions with  $n = 6$  and  $7$ , respectively. For clarity, the most important states are labeled, and the arrows represent the potential laser excitation process for the optical pumping experiment (see the Text for details).

dipole ( $M1$ ) transition probabilities for the Rf<sup>+</sup> ion, using the effective Hamiltonian. The intraconfiguration  ${}^2D_{3/2} \rightarrow {}^2D_{5/2}$  transition is magnetic dipole allowed. By using the Supplemental Material Eq. (S4) [31] as a function of the tabulated Einstein coefficient we obtain a lifetime of 0.7 s for the excited  ${}^2D_{5/2}$  state ( $6d^1 7s^2$ ). The intraconfiguration  ${}^4F \rightarrow {}^4F$  transitions are also magnetic dipole allowed with the corresponding Einstein coefficients on the order of  $0.1 s^{-1}$ . The interconfiguration  ${}^2D_{3/2} \rightarrow {}^4F$  transitions are *a priori* electric quadrupole allowed, whereas for the  ${}^2D_{3/2} \rightarrow {}^4F_{3/2}$  the contributions from both  $M1$  and  $E2$  channels are more or less of the same magnitude. Based on this information, we derive a lifetime of about 20 s for the metastable  ${}^4F_{3/2}$  state ( $6d^2 7s^1$ ). The calculated lifetimes of the  ${}^4F_{5/2}$  and  ${}^4F_{7/2}$  states ( $6d^2 7s^1$ ) equal 6 and 282 s, respectively.

### C. Optical pumping scheme

In Fig. 1 we present the energy diagrams of Hf<sup>+</sup> and Rf<sup>+</sup> in the range of 0 to 30 000  $cm^{-1}$ . We observe a much less dense landscape of energy levels for the heavier atom, which enables the development of efficient pumping schemes for LRC experiments. For the Hf<sup>+</sup> ion, a potential LRC approach would involve pumping the ground-state  ${}^2D_{3/2}$  (configuration  $5d^1 6s^1$ ) to the bright  ${}^4F_{3/2}$  ( $5d^1 6s^1 6p^1$ ) odd-parity level [3,5]. The excited state radiatively decays *via* two processes, reaching either the ground-state [ ${}^4F_{3/2}$  ( $5d^1 6s^1 6p^1$ )  $\rightarrow$   ${}^2D_{3/2}$  ( $5d^1 6s^1$ )] or the metastable state [ ${}^4F_{3/2}$  ( $5d^1 6s^1 6p^1$ )  $\rightarrow$   ${}^4F_{3/2}$  ( $5d^2 6s^1$ )], marked by the gray arrow in Fig. 1(a) with a sizable branching ratio (see also Table IV). Since LRC exploits ion drift in dilute gases and because the energy separation between the metastable state and the lowest excited state of Hf<sup>+</sup> is small, we expect the metastable state to

decay predominantly by collisional quenching due to competing intersystem crossing.

To enable LRC on the  $\text{Rf}^+$  ion, we propose two different approaches based on the obtained energy levels where the metastable state  $^4F_{3/2}$  (configuration  $6d^27s^1$ ) that has a radiative lifetime of 20 s is selectively targeted. The first approach that is marked with the gray arrow in Fig. 1(b) is similar to that for  $\text{Hf}^+$  where pumping the ground-state  $^2D_{3/2}$  ( $6d^17s^2$ ) to the bright  $^4F_{3/2}$  ( $6d^17s^17p^1$ ) odd-parity level effectively feeds the metastable  $^4F_{3/2}$  ( $6d^27s^1$ ) state with a significant branching ratio (see also Table V). The second approach that is marked with the yellow arrow in Fig. 1(b) involves pumping of the ground state to the  $^2P_{1/2}$  ( $7s^27p^1$ ) odd-parity level. In this scenario, the branching ratio to the metastable state is rather small (see Table V). But since our calculations predict the ( $7s^27p^1$ ) level to lie very close above the metastable state, we expect collisional quenching to be very efficient and to dominate the pumping process.

#### IV. CONCLUSIONS

In this paper, we report a theoretical investigation of the electronic structure and spectroscopic properties of the  $\text{Rf}^+$  ion. The results are obtained using the state-of-the-art four-component relativistic MRCI calculation. We use an effective Hamiltonian approach in conjunction with the *ab initio* calculations to estimate the transition probabilities for the various interconfigurational and intraconfigurational electron transitions beyond the electric dipole approximation. We also present the energy spectrum of the lighter homolog  $\text{Hf}^+$  ion. For this system, the calculated energy levels and spectroscopic properties are in good agreement with the reported experimental data, confirming the suitability of the MRCI model for this

paper. Thus, we expect comparable quality of the prediction for the SHE  $\text{Rf}^+$  ion.

For  $\text{Rf}^+$ , the calculated energy spectrum is less dense than that obtained for the lighter homolog, suggesting an electronic structure that is primarily governed by the strong relativistic spin-orbit coupling interaction. Our results are consistent with the earlier studies, but we have also obtained the energy levels of the metastable states that arise from configuration  $6d^27s^1$  and the lifetimes of the various levels. In addition, the presented method will be relevant for studying also the  $\text{Rf}^+$ -He interaction potential that constitutes the next step in our future investigation.

Based on our calculations, we propose two possible excitation schemes to enable LRC on the  $\text{Rf}^+$  ion. The first scheme involves pumping the ground-state  $^2D_{3/2}$  (configuration  $6d^27s^1$ ) to the bright excited-state  $^4F_{3/2}$  (configuration  $6d^17s^17p^1$ ) in the ultraviolet energy range (330 nm), which effectively feeds the lowest metastable  $^4F_{3/2}$  state (configuration  $6d^27s^1$ ). The second involves pumping the ground state to the bright excited-state  $^2P_{1/2}$  (configuration  $7s^27p^1$ ) in the visible energy range (600 nm), eventually reaching the metastable state via possible collisional quenching.

#### ACKNOWLEDGMENTS

This project has received funding from the European Research Council (ERC) under the European Union's Horizon 2020 Research and Innovation Programme (Grant Agreement No. 819957). We also gratefully acknowledge high performance computing (HPC) support, time and infrastructure from : the Center for Information Technology of the University of Groningen (Peregrine), the Johannes Gutenberg University of Mainz (Mogon), and the HPC group of GSI.

- 
- [1] R. Eichler, *Nucl. Phys. News* **29**, 11 (2019).
- [2] P. Schwerdtfeger, O. R. Smits, and P. Pyykkö, *Nat. Rev. Chem.* **4**, 359 (2020).
- [3] M. Laatiaoui and S. Raeder, *Nucl. Phys. News* **29**, 21 (2019).
- [4] M. Block, M. Laatiaoui, and S. Raeder, *Prog. Part. Nucl. Phys.* **116**, 103834 (2021).
- [5] M. Laatiaoui, A. A. Buchachenko, and L. A. Viehland, *Phys. Rev. Lett.* **125**, 023002 (2020).
- [6] M. Laatiaoui, H. Backe, D. Habs, P. Kunz, W. Lauth, and M. Sewtz, *Eur. Phys. J. D* **66**, 232 (2012).
- [7] M. Laatiaoui, A. A. Buchachenko, and L. A. Viehland, *Phys. Rev. A* **102**, 013106 (2020).
- [8] E. V. Kahl, J. C. Berengut, M. Laatiaoui, E. Eliav, and A. Borschevsky, *Phys. Rev. A* **100**, 062505 (2019).
- [9] P. Indelicato, J. Bieroń, and P. Jönsson, *Theor. Chem. Acc.* **129**, 495 (2011).
- [10] U. Kaldor and E. Eliav, *Adv. Quantum Chem.* **31**, 313 (1998).
- [11] W. C. Martin and J. Sugar, *Phys. Rev. A* **53**, 1911 (1996).
- [12] E. Johnson, B. Fricke, O. L. Keller, C. W. Nestor, and T. C. Tucker, *J. Chem. Phys.* **93**, 8041 (1990).
- [13] V. Pershina and B. Fricke, *J. Phys. Chem.* **98**, 6468 (1994).
- [14] W. Liu, R. Franke, and M. Dolg, *Chem. Phys. Lett.* **302**, 231 (1999).
- [15] J. Anton, M. Hirata, B. Fricke, and V. Pershina, *Chem. Phys. Lett.* **380**, 95 (2003).
- [16] V. Pershina, A. Borschevsky, M. Iliaš, and A. Türler, *J. Chem. Phys.* **141**, 064315 (2014).
- [17] E. Eliav, U. Kaldor, and Y. Ishikawa, *Phys. Rev. Lett.* **74**, 1079 (1995).
- [18] DIRAC, a relativistic *ab initio* electronic structure program, Release DIRAC19 (2019), written by A. S. P. Gomes, T. Saue, L. Visscher, H. J. A. Jensen, and R. Bast, with contributions from I. A. Aucar, V. Bakken, K. G. Dyall, S. Dubillard, U. Ekström, E. Eliav, T. Enevoldsen, E. Faßhauer, T. Fleig, O. Fossgaard, L. Halbert, E. D. Hedegård, B. Heimlich-Paris, T. Helgaker, J. Henriksson, M. Iliaš, C. R. Jacob, S. Knecht, S. Komorovský, O. Kullie, J. K. Lærdahl, C. V. Larsen, Y. S. Lee, H. S. Nataraj, M. K. Nayak, P. Norman, G. Olejniczak, J. Olsen, J. M. H. Olsen, Y. C. Park, J. K. Pedersen, M. Pernpointner, R. di Remigio, K. Ruud, P. Salek, B. Schimmelpfennig, B. Senjean, A. Shee, J. Sikkema, A. J. Thorvaldsen, J. Thyssen, J. van Stralen, M. L. Vidal, S. Villaume, O. Visser, T. Winther, and S. Yamamoto, available at <http://www.diracprogram.org>.
- [19] P. Parmar, K. A. Peterson, and A. E. Clark, *J. Phys. Chem. A* **117**, 11874 (2013).



- [20] D. H. Bross, P. Parmar, and K. A. Peterson, *J. Chem. Phys.* **143**, 184308 (2015).
- [21] A. Kovács, R. J. M. Konings, J. K. Gibson, I. Infante, and L. Gagliardi, *Chem. Rev.* **115**, 1725 (2015).
- [22] J. Desclaux, *Comput. Phys. Commun.* **9**, 31 (1975).
- [23] C. Froese Fischer, G. Gaigalas, P. Jönsson, and J. Bieroń, *Comput. Phys. Commun.* **237**, 184 (2019).
- [24] E. Kahl and J. Berengut, *Comput. Phys. Commun.* **238**, 232 (2019).
- [25] S. Fritzsche, *Comput. Phys. Commun.* **240**, 1 (2019).
- [26] G. Visentin, M. Laatiaoui, L. A. Viehland, and A. A. Buchachenko, *Front. Chem.* **8**, 438 (2020).
- [27] NIST ASD Team, A. Kramida, Y. Ralchenko, and J. Reader, NIST Atomic Spectra Database (ver. 5.8). Available: <https://physics.nist.gov/asd> [2017, April 9]. (National Institute of Standards and Technology, Gaithersburg, MD 2020).
- [28] L. Visscher and K. G. Dyall, *At. Data Nucl. Data Tables* **67**, 207 (1997).
- [29] K. G. Dyall, *Theor. Chem. Acc.* **112**, 403 (2004).
- [30] K. G. Dyall, *Theor. Chem. Acc.* **129**, 603 (2011).
- [31] See Supplemental Material at <http://link.aps.org/supplemental/10.1103/PhysRevA.104.022813> for selective equations for the calculation of Einstein Coefficients as function of transition probabilities; Calculated energy levels of Hf<sup>+</sup> as function of the basis set expansion and the GAS set-ups; Calculated energy levels of Hf<sup>+</sup> and Rf<sup>+</sup>: MRCI versus effective Hamiltonian model; Graphical representations of the calculated absorption spectra of Hf<sup>+</sup> and Rf<sup>+</sup>: MRCI versus effective Hamiltonian model.
- [32] M. S. Safronova, A. Derevianko, and W. R. Johnson, *Phys. Rev. A* **58**, 1016 (1998).
- [33] R. E. Stanton and S. Havriliak, *J. Chem. Phys.* **81**, 1910 (1984).
- [34] T. Saue, R. Bast, A. S. P. Gomes, H. J. A. Jensen, L. Visscher, I. A. Aucar, R. Di Remigio, K. G. Dyall, E. Eliav, E. Fasshauer *et al.*, *J. Chem. Phys.* **152**, 204104 (2020).
- [35] J. C. Slater, *Quantum Theory of Atomic Structure*, International Series of Monographs on Physics Vols. 1 and 2 (McGraw-Hill, New York, 1960).
- [36] J. Thyssen, T. Fleig, and H. J. A. Jensen, *J. Chem. Phys.* **129**, 034109 (2008).
- [37] S. Knecht, H. J. A. Jensen, and T. Fleig, *J. Chem. Phys.* **132**, 014108 (2010).
- [38] T. Fleig, J. Olsen, and L. Visscher, *J. Chem. Phys.* **119**, 2963 (2003).
- [39] T. Fleig, *Chem. Phys.* **395**, 2 (2012).
- [40] T. Fleig and M. K. Nayak, *Phys. Rev. A* **88**, 032514 (2013).
- [41] J. E. Sansonetti and W. C. Martin, *J. Phys. Chem. Ref. Data* **34**, 1559 (2005).
- [42] P. Indelicato, J. P. Santos, S. Boucard, and J.-P. Desclaux, *Eur. Phys. J. D* **45**, 155 (2007).
- [43] K. Dyllal, I. Grant, C. Johnson, F. Parpia, and E. Plummer, *Comput. Phys. Commun.* **55**, 425 (1989).
- [44] P. Jönsson, X. He, C. Froese Fischer, and I. Grant, *Comput. Phys. Commun.* **177**, 597 (2007).
- [45] L. F. Pašteka, E. Eliav, A. Borschevsky, U. Kaldor, and P. Schwerdtfeger, *Phys. Rev. Lett.* **118**, 023002 (2017).
- [46] S. Fritzsche, *Eur. Phys. J. D* **33**, 15 (2005).
- [47] S. Fritzsche, C. Z. Dong, F. Koike, and A. Uvarov, *Eur. Phys. J. D* **45**, 107 (2007).
- [48] E. Eliav, U. Kaldor, and Y. Ishikawa, *Phys. Rev. A* **49**, 1724 (1994).
- [49] E. Eliav, U. Kaldor, and Y. Ishikawa, *Phys. Rev. A* **50**, 1121 (1994).
- [50] B. R. Judd, *Operator Techniques in Atomic Spectroscopy* (McGraw-Hill, New York, 1963).
- [51] R. D. Cowan, *The Theory of Atomic Structure and Spectra* (University of California Press, Oakland, CA, 1981).
- [52] A. A. Misetich and T. Buch, *J. Chem. Phys.* **41**, 2524 (1964).
- [53] H. Ramanantoanina, *J. Chem. Phys.* **149**, 054104 (2018).
- [54] T. N. Poe, M. J. Beltrán-Leiva, C. Celis-Barros, W. L. Nelson, J. M. Sperling, R. E. Baumbach, H. Ramanantoanina, M. Speldrich, and T. E. Albrecht-Schönzart, *Inorg. Chem.* **60**, 7815 (2021).
- [55] H. Ramanantoanina, *Phys. Chem. Chem. Phys.* **19**, 32481 (2017).
- [56] H. Ramanantoanina and M. Gruden, *Int. J. Quantum Chem.* **120**, e26081 (2020).
- [57] T. E. Albrecht-Schmitt, D. E. Hobart, D. Páez-Hernández, and C. Celis-Barros, *Int. J. Quantum Chem.* **120**, e26254 (2020).
- [58] MATLAB, *version 8.5.0 (R2015a)* (The MathWorks, Inc., Natick, MA, 2015).